



## Removal of dissolved inorganic phosphorus with modified gravel sand: kinetics, equilibrium, and thermodynamic studies

Wei Huang, Liangjie Zhang, Junqi Gao, Jihua Li, Jibiao Zhang\*, Zheng Zheng\*

*Department of Environmental Science and Engineering, Fudan University, Shanghai 200433, P.R. China,*

*Tel./Fax: +86 21 65642948; emails: yixinghd6@163.com (W. Huang), 605909131@qq.com (L. Zhang), 173676749@qq.com (J. Gao), 12110740007@fudan.edu.cn (J. Li), jbzhang@fudan.edu.cn (J. Zhang), zzhenghj@fudan.edu.cn (Z. Zheng)*

Received 17 April 2014; Accepted 21 October 2014

### ABSTRACT

The sorption of dissolved inorganic phosphorus by modified gravel sand (iron-doped and calcined gravel sand) was studied through kinetic, equilibrium, and thermodynamic experiments. The maximum phosphorus sorption capacity of iron-doped and calcined gravel sand was 1.01 and 2.93 mg g<sup>-1</sup>, respectively. When the solution pH gradually approached a highly alkaline condition, the phosphorus removal efficiency of iron-doped gravel sand decreased sharply and that of calcined gravel sand increased. With an increase in initial phosphorus concentration, the sorption capacity of calcined gravel sand increased significantly (0.8–3.1 mg g<sup>-1</sup>), and that of iron-doped gravel sand was relatively constant (1.2 mg g<sup>-1</sup>). Data from the isotherm experiments were well described by Langmuir isotherm model. Kinetic studies illustrated that the rate of sorption followed both the pseudo-first-order and pseudo-second-order models, and that the pseudo-second-order model could better describe the sorption kinetics. The calculated thermodynamic parameters suggested that the sorption was a feasible or spontaneous ( $\Delta G < 0$ ), entropy-driven ( $\Delta S > 0$ ), and endothermic ( $\Delta H > 0$ ) reaction.

*Keywords:* Gravel sand; Phosphorus removal; Sorption; Isotherm; Kinetics; Thermodynamic

### 1. Introduction

As an essential element for the growth of organisms, phosphorus (P) is present in soils, sediments, waters, and organisms [1,2]. However, excessive phosphorus entering into rivers or lakes can cause eutrophication, the disordered growth of undesirable algae, and other aquatic plants [3], which has become a widespread environmental problem. As more and more stringent regulations are implemented, reduction or removal of phosphorus in polluted water is becoming one of the most important tasks in wastewater

treatment [4]. Dissolved inorganic phosphorus (DIP) or orthophosphate is considered to be the only form which can be directly utilized and rapidly assimilated by bacteria, algae [5], and plants [6]. Therefore, DIP must be targeted for removal if the problem of eutrophication is to be addressed, and new materials or methods should be studied. Some cost-effective phosphorus removal methods were introduced in early studies. Soils, slags, zeolite, and calcite appear to be promising candidates to remove phosphorus in water [7–9]. Several studies have indicated that some filtration materials such as sand and burned clay coated with oxides of iron, aluminum, or manganese act as good sorbents [10–12]. Furthermore, plant residuals

\*Corresponding authors.

such as date palm fibers [13] and *Poseidonia oceanica* fibers [14,15] have been tested as materials of phosphorus removal. Though most of them are used in different on-site solutions, such as sand filters, wetland systems, and some experimental projects [16,17], it is still difficult to remove phosphorus of high concentration efficiently [18] and economically in these small-scale on-site systems. Consequently, more attention should be paid to cost-efficient materials for removing phosphorus from wastewater.

Gravel of different sizes is widely used as a general filter material in wastewater treatment [19]. However, DIP sorption to gravel was seldom reported due to its low phosphorus removal efficiency. In this study, we analyzed two new kinds of materials prepared with gravel: iron-doped gravel sand and calcined gravel sand. Consequently, it is important to understand the reaction mechanism between DIP and sorbents for modeling its movement and fate in sewage treatment systems. The study aims to research the feasibility and mechanism of DIP removal with gravel sand and to compare the sorption efficiencies of two new materials under various conditions. Sorption equilibrium conditions, isotherms, kinetics, and thermodynamic parameters were evaluated in batch experiments. Scanning electron microscope (SEM), nitrogen adsorption analysis, X-ray diffraction (XRD), X-ray fluorescence (XRF), and infrared spectroscopy (FTIR) were used to characterize these two new materials. Some new insights into DIP removal with gravel sand were discovered in this study, and this work also initially evaluated the future engineering applications of iron-doped gravel sand and calcined gravel sand.

## 2. Material and methods

### 2.1. Sorption materials

Unprocessed gravel was supplied by a material factory in Zhengzhou, China. The samples rinsed with distilled water were comminuted with mill, sieved (<0.12 mm), and named as G. Afterwards, 2.0 g of the raw sample was added to 200 mL of 0.2 mol L<sup>-1</sup>/FeSO<sub>4</sub> solution to modify the samples (G), and then the mixture was stirred for 12 h at room temperature. Then the modified samples were obtained by filtration and drying and named as G-Fe. Other raw samples (G) were calcined in a muffle furnace. The temperature increased from room temperature (25 ± 2 °C) to 800 °C, and the samples were calcined at 800 °C for 2 h in aerobic conditions which could be used to avoid the carbonization phenomenon. The cooled calcined gravel sand samples (named as G-C) were obtained.

### 2.2. Phosphorus compounds

Potassium dihydrogen phosphate (KH<sub>2</sub>PO<sub>4</sub>) was selected to prepare DIP solution for the experiments. The DIP concentration in the solution was determined by the molybdenum blue method after the solution was filtered (0.45 μm filtration membrane) [20].

### 2.3. Characterization of materials

SEM (Philips XL 30) was used to examine the surface morphology and structure of gravel sand samples. Specific surface area was measured by N<sub>2</sub> adsorption method with the Micromeritics Tristar 3000 Surface Analyzer in the relative pressure range of 0.001–0.995 atmospheres. Chemical composition of the samples was determined by XRF analyzer (S4 EXPLORER, Germany). XRD analysis instrument (D8 Advance, Germany) was utilized to analyze the mineralogy of gravel sand samples. The surface functional groups were identified according to transmission infrared spectra obtained from a Fourier transform infrared (FTIR) spectrophotometer (Nicolet 6700, USA).

### 2.4. Sorption isotherm experiments

The sorption isotherms experiments were conducted at 25, 35, and 45 °C. Samples (0.3 g) were added to a series of 150-mL beaker flasks containing 50 mL DIP solutions with various P concentrations (0, 5, 10, 15, 20, 25, and 30 mg L<sup>-1</sup>). The beaker flasks were shaken in a temperature-controlled shaker at a speed of 220 rpm under the various constant temperatures. After 75 min, the solution was filtered (0.45 μm filtration membrane) for DIP analysis [21].

### 2.5. Kinetics sorption experiments

Batched experiments were carried out to evaluate the kinetics of DIP sorption. Samples (0.3 g) were added into 50 mL of 20 mg L<sup>-1</sup> DIP solution. Samples were shaken in a temperature-controlled shaker under various constant temperatures of 25, 35, and 45 °C at a speed of 220 rpm in batches. The equilibration time used to evaluate the sorption kinetics is 1, 2, 4, 6, 10, 14, 30, 45, and 75 min.

### 2.6. Thermodynamic parameters

Samples (0.3 g) were added into 50 mL DIP solutions with various initial concentrations (5, 10, 15, 20, 25, and 30 mg L<sup>-1</sup>) at three different temperatures: 25,

35, and 45°C. Batch samples were shaken in a temperature-controlled shaker for 75 min. The thermodynamic parameters of DIP sorption, such as enthalpy ( $\Delta H$ ), Gibbs energy ( $\Delta G$ ), and entropy ( $\Delta S$ ), were estimated by fitting linear equations to the thermodynamic data obtained under different concentrations.

### 3. Results and discussion

#### 3.1. Characterization of the gravel sand

##### 3.1.1. Physical property

According to the measurements by  $N_2$  adsorption method with the Micromeritics Tristar 3000, the specific surface area of raw gravel sand (G) was  $4.07 \text{ m}^2 \text{ g}^{-1}$  with a total pore volume of  $9.52 \times 10^{-4} \text{ cm}^3 \text{ g}^{-1}$  (Table 1). The iron-doped sample (G-Fe) had the higher specific surface area ( $11.03 \text{ m}^2 \text{ g}^{-1}$ ) and total pore volume ( $4.22 \times 10^{-3} \text{ cm}^3 \text{ g}^{-1}$ ) than raw gravel sand. The difference could be interpreted as follows: the raw gravel had poor internal volume and doped iron in iron-doped gravel sand increased the specific surface area or pore volume [22]. The calcined gravel sand (G-C) showed a low specific surface area of  $1.79 \text{ m}^2 \text{ g}^{-1}$  with a total pore volume of  $3.32 \times 10^{-4} \text{ cm}^3 \text{ g}^{-1}$ , indicating that the more concentrated mesopores and macropores were generated due to the microporous occlusion and subsidence damage of gravel sand [23].

The mineralogical composition is provided in Table 1. Obviously, the iron-doped gravel sand had the higher content of Fe (2.77%) and the lower Ca content than other kinds of gravel sand. Ion exchange between Fe and Ca might occur during the modification process and might attribute to the sorption efficiency of iron-doped gravel sand.

##### 3.1.2. Morphology analysis

SEM analysis was conducted to explore the internal structure and morphology of gravel sand samples. The raw gravel sand had a smooth and flat surface

(Fig. 1(a)). A large number of pores observed on the iron-doped gravel sand surface (Fig. 1(b)) increased the surface area and pore volume, and the surface structure was more conducive to sorption [24]. Due to the occlusion and subsidence damage of the gravel sand surface, a porous structure was formed in calcined gravel sand after calcinations (Fig. 1(c)).

##### 3.1.3. XRD analysis

XRD was utilized to identify the material morphological structure with a non-quantitative description [25]. The XRD diagrams are shown in Fig. 2. The diagrams of iron-doped gravel sand (G-Fe) and calcined gravel sand (G-C) were almost the same, indicating that they had the same mineralogy. In Fig. 2(a), a new peak could be observed at  $29.40^\circ$ , indicating that the raw sample might have the crystal form of calcite according to the data from the Joint Committee on Powder Diffraction Standards (JCPDS pattern number: 41-1475). No peak occurred at  $29.40^\circ$  in Fig. 2(b) and (c) due to the modification and calcinations.

##### 3.1.4. FTIR analysis

Fig. 3 showed the FTIR spectra of the gravel sand samples. The clear distinctions were observed in the FTIR spectra of raw gravel sand (G), iron-doped gravel sand (G-Fe), and calcined gravel sand (G-C). The peak at  $1,125 \text{ cm}^{-1}$  in G-Fe and G corresponded to the stretching and vibration of Si-O-Fe, and a strong Ca-O-Fe peak at  $1,050 \text{ cm}^{-1}$  which only existed in G-C illustrated that Ca took part in the sorption with Fe [26]. The peak around  $875 \text{ cm}^{-1}$  (existed in G-Fe and G) might be assigned to the Fe-C or Ca-C [27], and no peak existed in G-C due to the cleavage of Fe-C or Ca-C bonds during calcination. Additionally, the peak at  $780 \text{ cm}^{-1}$  could be assigned to the Fe-OH in three materials [28]. After all, hydrogen bonding was not the main mechanism of the sorption process for G-C and G-Fe, since the modified gravel sand must be clouded with water molecules and is

Table 1  
Physical property of gravel sand samples

Sorbents	Surface property analysis		Elemental analysis (%)				
	Specific surface area ( $\text{m}^2 \text{ g}^{-1}$ )	Pore volume ( $\text{cm}^3 \text{ g}^{-1}$ )	Si	Fe	Al	Mg	Ca
G	4.07	$9.52 \times 10^{-4}$	25.90	0.97	1.77	0.42	2.08
G-Fe	11.03	$4.22 \times 10^{-3}$	24.10	2.77	1.45	0.13	0.20
G-C	1.79	$3.32 \times 10^{-4}$	26.00	1.09	1.71	0.62	2.25

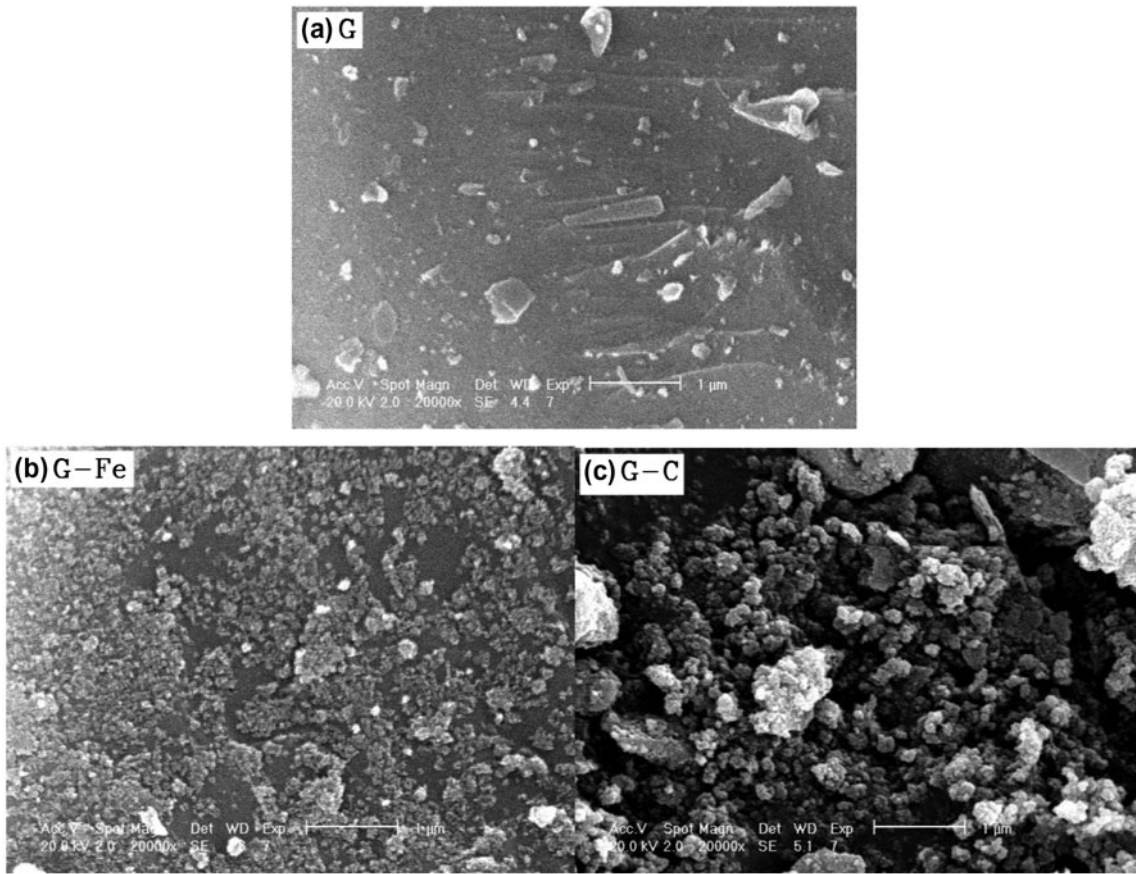


Fig. 1. SEM images of gravel sand samples ((a) for G, (b) for G-Fe, and (c) for G-C).

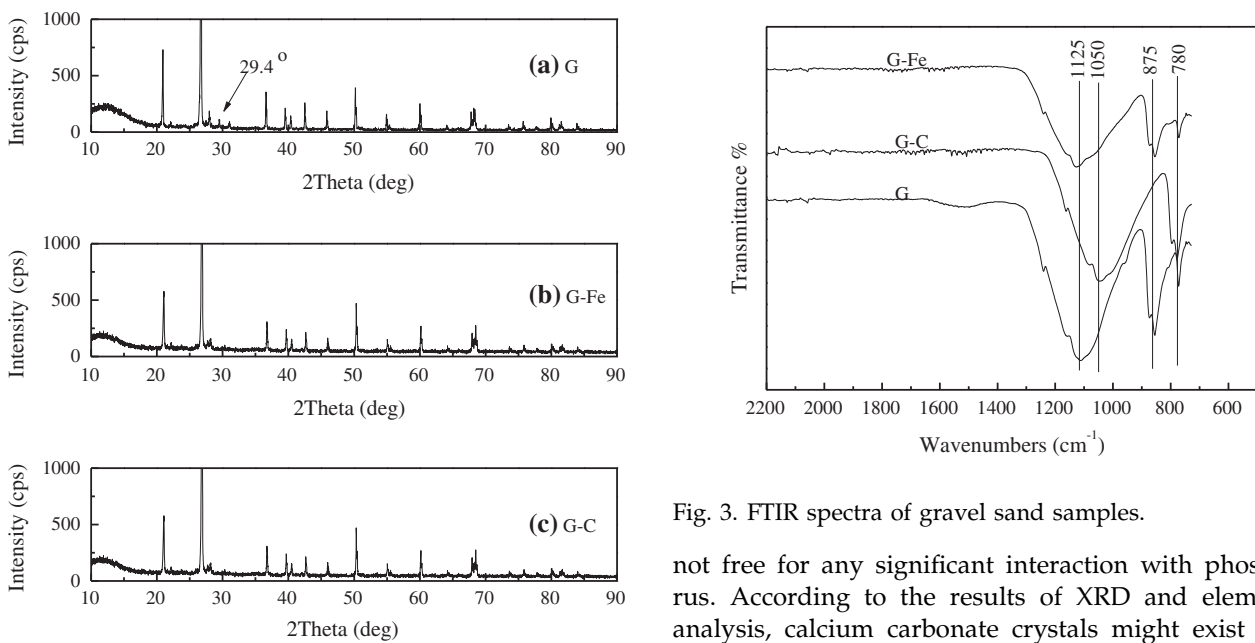


Fig. 3. FTIR spectra of gravel sand samples.

Fig. 2. XRD patterns of gravel sand samples ((a) for G, (b) for G-Fe, and (c) for G-C).

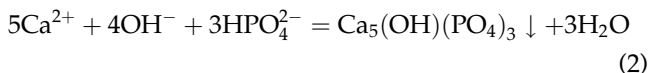
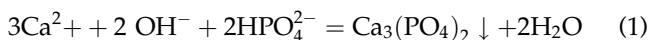
not free for any significant interaction with phosphorus. According to the results of XRD and elemental analysis, calcium carbonate crystals might exist in G and G-Fe. The iron-doped gravel sand might supply new sites for sorption and the sorption process of calcined gravel sand was not a simple physical process.

### 3.2. Equilibrium studies

#### 3.2.1. Effect of pH on percentage removal of DIP

As shown in Fig. 4, the removal percentage of DIP was highly affected by pH. The results indicated that the calcined gravel sand (G-C) had the higher removal efficiency than the other two materials in different pH conditions. As the pH of the solution approached a highly alkaline condition (pH 11.02), the removal efficiency of raw gravel sand (G) increased slightly from 14 to 25% and calcined gravel sand (G-C) increased from 68 to 91%. On the contrary, when the pH of the solution was increased from 3.18 to 11.02, the removal efficiency of iron-doped gravel sand decreased from 52 to 25%.

When pH increased,  $\text{H}_2\text{PO}_4^-$  was dissociated to  $\text{HPO}_4^{2-}$  to react with  $\text{Ca}^{2+}$  to generate non-crystal calcium phosphate ( $\text{Ca}_3(\text{PO}_4)_2$ ) due to the high content of calcium in raw gravel sand (G) and calcined gravel sand (G-C). Furthermore,  $\text{Ca}_3(\text{PO}_4)_2$  could be converted to the stable  $\text{Ca}_5(\text{OH})(\text{PO}_4)_3$  (HAP). Therefore, the removal efficiency increased with pH rise. The reactions were provided as follows:



In iron-doped gravel sand (G-Fe), the electrostatic properties might be influenced by pH. When pH increased,  $\text{OH}^-$  competed with phosphate for the active sites on the surfaces of sorbents, thus affecting the sorption efficiency [29]. Additionally, the pH-

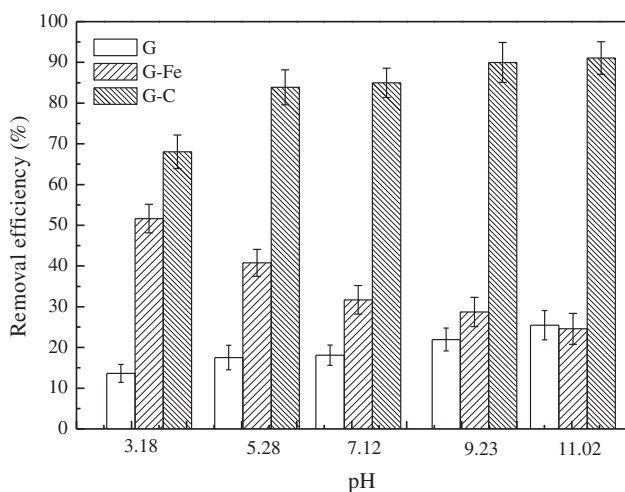


Fig. 4. Effect of pH on the removal of DIP.

dependent phosphorus removal efficiency might be associated with ligand exchange between  $\text{OH}^-$  and P [30], and the high content of Fe in iron-doped gravel sand supplied the condition for ligand exchange. The reactions were provided as

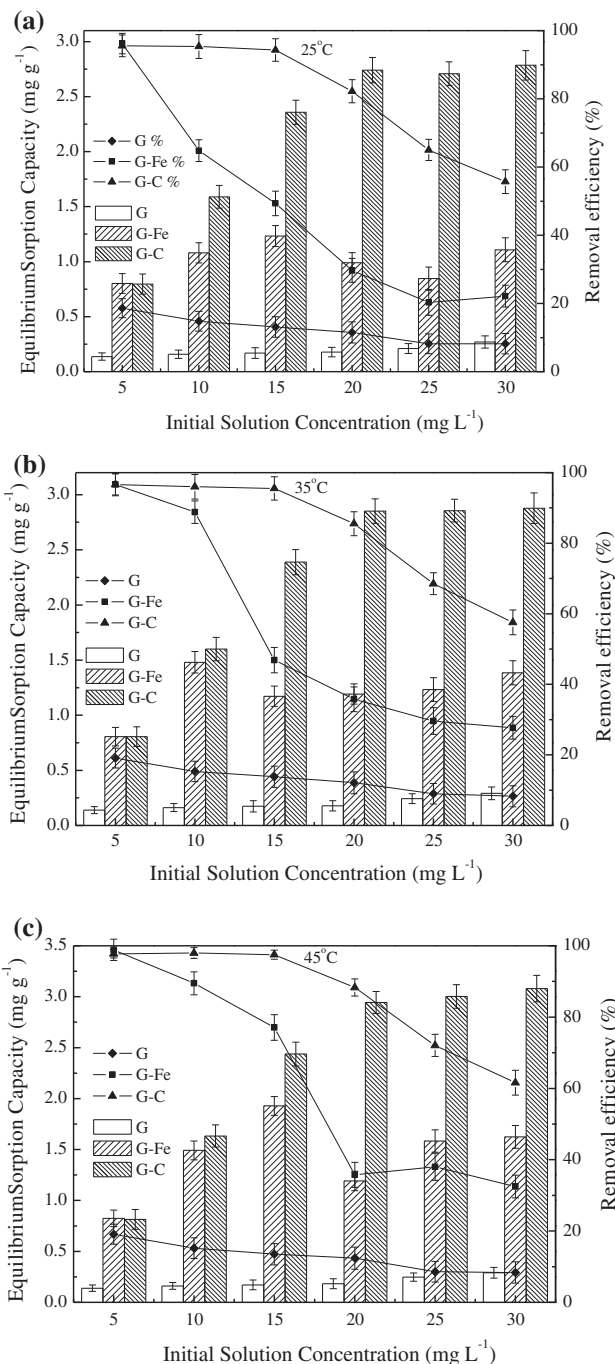
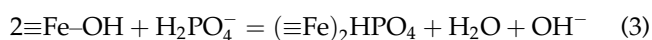


Fig. 5. Effect of initial concentration on the DIP removal at various temperatures ((a) 25°C; (b) 35°C; and (c) 45°C).



### 3.2.2. Effect of initial concentration on the removal of DIP in different temperatures

The effect of initial concentration on the removal of DIP with raw gravel sand (G), iron-doped gravel sand (G-Fe), and calcined gravel sand (G-C) at three different temperatures (25, 35, and 45°C) was studied. The equilibrium sorption capacity  $q_e$  ( $\text{mg g}^{-1}$ ) and phosphorus removal efficiency ( $\eta\%$ ) were used to describe the removed phosphorus removal, and Fig. 5 showed the difference among these materials at the three temperatures. For example, at 25°C, the initial concentration had small effects on the removal efficiency of raw gravel sand. The removal efficiency of iron-doped gravel sand decreased rapidly (96–30%) when the initial phosphorus concentration increased from 5 to 20  $\text{mg L}^{-1}$ , and then the removal efficiency tended to be balanced (30–22%). This observation could be explained as follows: all sites on the surface were vacant and the available sorption sites decreased rapidly and when almost all the available sites were fully utilized, the removal efficiency tended to be balanced [31]. Additionally, the phosphorus removal efficiency of calcined gravel sand was stable (around 95%) when the initial concentration increased from 5 to 15  $\text{mg L}^{-1}$  and then decreased significantly (94–55%). Chemical sorption might occur due to the morphological change of calcium and when the initial concentration increased, the amount of calcium decreased and the removal efficiency decreased significantly.

At these different temperatures, the initial concentration had small effects on the equilibrium sorption capacity of raw gravel sand (G). When the tempera-

ture and initial concentration increased, the equilibrium sorption capacity of iron-doped gravel sand increased slowly and was relatively constant (approximately 1.2  $\text{mg g}^{-1}$ ), since the available site on the surface was limited. The equilibrium sorption capacity of calcined gravel sand (G-C) was larger (up to 3.08  $\text{g mg}^{-1}$  in 45°C) than that of iron-doped gravel sand (G-Fe), and the sorption capacity increased with the increase of initial concentration. The difference could be explained as follows: when the initial concentration was increased, the concentration gradient between adsorbent and adsorbate was increased and the probability of the contact between sorbent and sorbate was increased [32,33].

### 3.3. Sorption isotherm fitting

The Langmuir isotherm constants,  $q_m$  and  $K$ , were calculated with the slope and intercept of the plot of  $C_e/q_e$  vs.  $C_e$  according to Eq. (4) and provided in Table 2

$$\frac{C_e}{q_e} = \frac{1}{q_m} C_e + \frac{1}{Kq_m} \quad (4)$$

where  $q_e$  ( $\text{mg g}^{-1}$ ) and  $C_e$  ( $\text{mg L}^{-1}$ ) were the equilibrium sorption capacity and the equilibrium concentration of DIP, respectively;  $q_m$  ( $\text{mg g}^{-1}$ ) was a predicted maximum sorption capacity;  $K$  ( $\text{L mg}^{-1}$ ) was the affinity of the sorbent for the sorbate.

The plot of  $\log q_e$  vs.  $\log C_e$  according to Eq. (5) resulted in a straight line with a slope  $1/n$  and an intercept  $\log K_F$  in the Freundlich isotherm shown in Table 2.

Table 2

Langmuir and Freundlich isotherm parameters of DIP sorption on gravel sand (calculated uncertainties are given in parentheses)<sup>a</sup>

Sorbent	T/°C	Langmuir			Freundlich		
		$q_m$ ( $\text{mg g}^{-1}$ )	$K$ ( $\text{L mg}^{-1}$ )	$R^2$	$1/n$	$K_F$ ( $\text{mg g}^{-1}$ )( $\text{L mg}^{-1}$ ) <sup>1/n</sup>	$R^2$
G-Fe	25	1.26 (0.06)	3.673 (0.270)	0.9903	0.06 (0.02)	0.882 (0.017)	0.8728
	35	1.32 (0.04)	2.154 (0.525)	0.9858	0.10 (0.01)	0.957 (0.012)	0.9506
	45	1.53 (0.07)	5.094 (0.789)	0.9496	0.13 (0.05)	1.339 (0.049)	0.6272
G-C	25	2.85 (0.01)	2.918 (0.036)	0.9988	0.28 (0.07)	1.558 (0.053)	0.7935
	35	2.95 (0.01)	3.724 (0.030)	0.9870	0.43 (0.14)	2.141 (0.069)	0.7410
	45	3.12 (0.01)	5.028 (0.016)	0.9996	0.07 (0.01)	2.657 (0.010)	0.8775

<sup>a</sup>Standard error propagation methods were used to calculate uncertainties in the observation, which accounted for the uncertainties of all measured quantities.

$$\log q_e = (1/n) \log C_e + \log K_F \quad (5) \quad q_t = q_e(1 - e^{-k_1 t}) \quad (7)$$

where  $K_F$  was defined as the sorption capacity of the sorbent. The  $1/n$  value, which ranged from 0 to 1, was a dimensionless factor which could be used to measure the sorption intensity or surface heterogeneity [34].

In this study, the isotherm data were fitted to the above two models by linear regression according to the method of least squares. The results of the phosphorus sorption isotherm experiments are shown in Table 2. A Langmuir model ( $R^2$  values of 0.9496–0.9996) could describe the DIP sorption isotherm better than Freundlich model ( $R^2$  values of 0.6272–0.9506). For Langmuir isotherm,  $q_m$  increased with rising temperature, indicating that chemical sorption occurred [34]. Furthermore,  $q_m$  of gravel sand by calcination (G–C) was much higher than that of gravel sand modified with Fe (G–Fe), indicating that G–C sample had larger maximum sorption capacity than G–Fe sample. For Freundlich isotherm, the values of  $1/n$  ranged from 0 to 1, indicating that the conditions were conducive to sorption [35].

In addition, we compared maximum sorption capacities for phosphate obtained in this study with other sorbents. The results indicated that the iron-doped and calcined gravel sand had the higher sorption capacities than the common sorption materials such as zeolite, ceramic sand, quart sand, and shale (the sorption capacities are 0.46, 0.51, 0.02, and 0.65  $\text{mg g}^{-1}$ , respectively) [36,37]. Furthermore, G–Fe and G–C also has the higher sorption capacities than the materials which contain iron and aluminum such as pyrrhotite and bauxite (the sorption capacities are 0.92 and 0.61  $\text{mg g}^{-1}$ , respectively) [36,38]. It was suggested that the iron-doped and calcined gravel sand were the effective sorbents for purification of wastewater containing phosphate.

### 3.4. Kinetics

The kinetic of the sorption was the most commonly described with pseudo-first-order and pseudo-second-order models [39].

The pseudo-first-order expression was generally described with the following Eq. (6) [40]:

$$\frac{dq_t}{dt} = k_1(q_e - q_t) \quad (6)$$

After integration and the application of the boundary conditions, for  $q_t=0$  at  $t=0$  and  $q_t=q_t$  at  $t=t$ , the integral from Eq. (7) becomes:

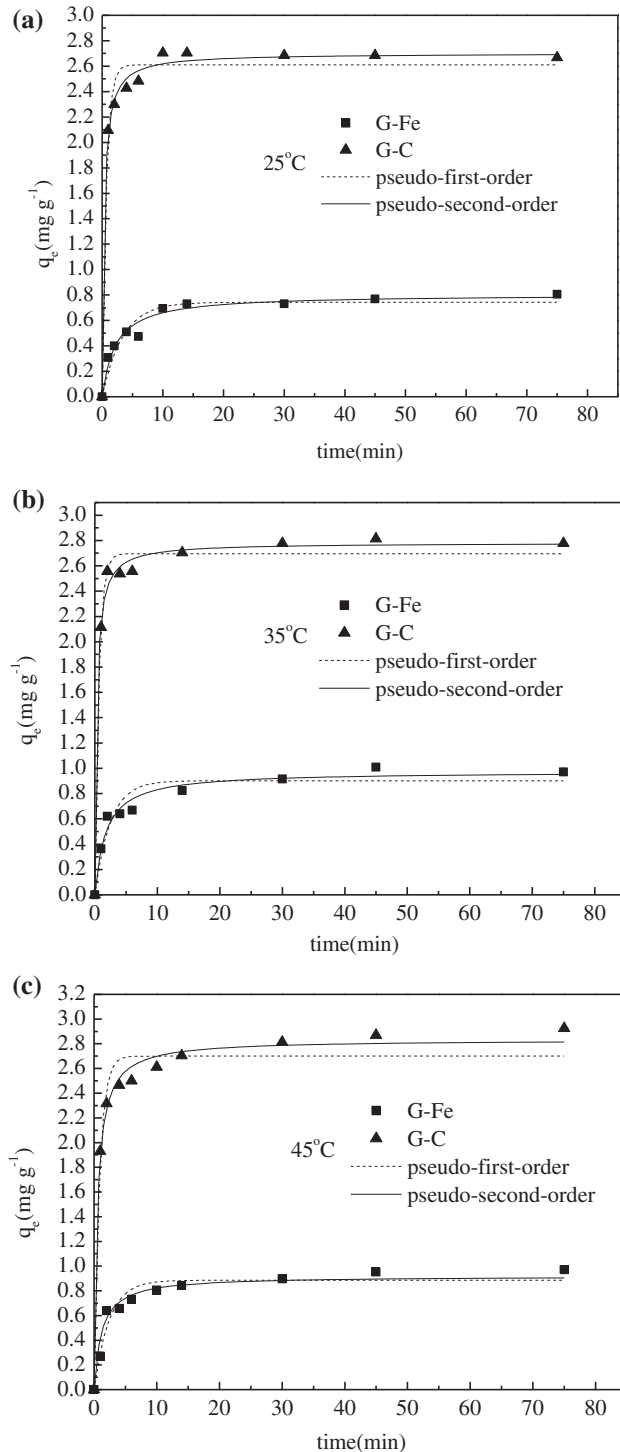


Fig. 6. Sorption kinetics of DIP onto G–C and G–Fe at various temperatures ((a) 25°C; (b) 35°C; and (c) 45°C).

Table 3

Fitting kinetics and mechanism parameters of DIP sorption onto G–C and G–Fe according to pseudo-first-order and pseudo-second-order models at three different temperatures (calculated uncertainties are given in parentheses)<sup>a</sup>

Sorbent	T/°C	$q_{\text{exp}}$ (mg g <sup>-1</sup> )	Pseudo-first-order			Pseudo-second-order		
			$q_e$ (mg g <sup>-1</sup> )	$k_1$ (min <sup>-1</sup> )	$R^2$	$q_e$ (mg g <sup>-1</sup> )	$k_2$ (g mg <sup>-1</sup> min <sup>-1</sup> )	$R^2$
G–Fe	25	0.81	0.74 (0.04)	0.298 (0.057)	0.9166	0.80 (0.03)	0.566 (0.121)	0.9615
	35	1.01	0.90 (0.05)	0.404 (0.090)	0.9028	0.97 (0.04)	0.596 (0.130)	0.9641
	45	0.97	0.89 (0.03)	0.418 (0.073)	0.9382	0.92 (0.01)	0.912 (0.053)	0.9531
G–C	25	2.69	2.61 (0.05)	1.469 (0.197)	0.9786	2.70 (0.03)	1.161 (0.145)	0.9949
	35	2.78	2.70 (0.04)	1.514 (0.169)	0.9876	2.78 (0.03)	1.231 (0.189)	0.9940
	45	2.93	2.70 (0.06)	1.134 (0.168)	0.9663	2.83 (0.04)	0.707 (0.088)	0.9923

<sup>a</sup>Standard error propagation methods were used to calculate uncertainties in the observation, which accounted for the uncertainties of all measured data.

where  $q_e$  and  $q_t$  were the amounts (mg g<sup>-1</sup>) of DIP adsorbed at equilibrium time and at time  $t$  (min), respectively;  $k_1$  was the first-order kinetics constant (min<sup>-1</sup>).

The pseudo-second-order equation was expressed as [41]:

$$\frac{t}{q_t} = \frac{1}{k_2 q_e^2} + \frac{t}{q_e} \quad (8)$$

where  $k_2$  was the second-order kinetics constant (g mg<sup>-1</sup> min<sup>-1</sup>).

Fig. 6 showed the kinetics of DIP sorption on the iron-doped gravel sand with Fe (G–Fe) and calcined gravel sand (G–C) with the curves predicted from pseudo-first-order and pseudo-second-order models, indicating that DIP sorption processes on the two kinds of samples were fast at the very beginning (10 min), but turned slow soon after the initial adsorption. And then, the amount of adsorbed DIP increased slowly to a plateau value in approximately 60 min. According to the comparison of the two materials, DIP sorption of calcined gravel sand was much larger than that of iron-doped gravel sand, and the relatively large value of  $q_e$  was obtained at 45°C. The rapid initial sorption could be interpreted as physical sorption mechanisms such as electrostatic interaction, in which the adhesion of phosphorus to the material surface occurred at the initial stage. The decreasing sorption rate thereafter could be attributed to ligand exchange [42].

In this study, the kinetic parameters of DIP were obtained through non-linear fitting with two models. The value of correlation coefficients ( $R^2$ ) indicated that both the pseudo-first-order and pseudo-second-order models could be used to fit the data and estimate model parameters ( $R^2 > 0.9$ ). But the overall data was

better fitted by pseudo-second-order model ( $0.9531 < R^2 < 0.9949$ ) for describing the sorption of DIP onto gravel sand samples, and the equilibrium sorption capacity ( $q_e$ ) was close to the experimental ones ( $q_{\text{exp}}$ ) obtained with the pseudo-second-order model. The rate constants ( $k$ ) of DIP sorption on the calcined gravel sand were higher than those on iron-

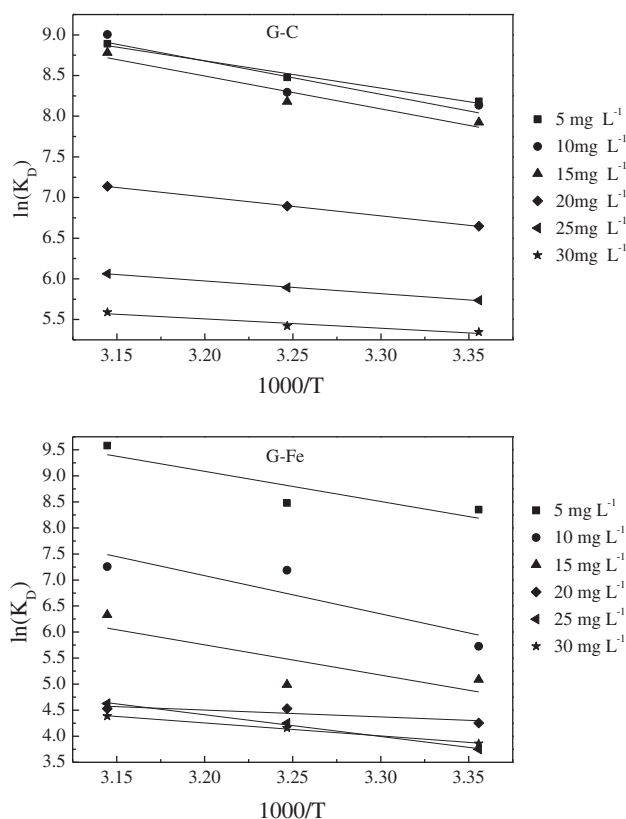


Fig. 7. Thermodynamic analysis for DIP sorption onto G–C and G–Fe.

Table 4  
Thermodynamic parameters for DIP sorption onto G–C and G–Fe

$C_0$ (mg L <sup>-1</sup> )	G–Fe					G–C				
	$\Delta H^\circ$ (kJ mol <sup>-1</sup> )	$\Delta S^\circ$ (kJ mol <sup>-1</sup> K <sup>-1</sup> )	$\Delta G^\circ$ (kJ mol <sup>-1</sup> )			$\Delta H^\circ$ (kJ mol <sup>-1</sup> )	$\Delta S^\circ$ (kJ mol <sup>-1</sup> K <sup>-1</sup> )	$\Delta G^\circ$ (kJ mol <sup>-1</sup> )		
			25°C	35°C	45°C			25°C	35°C	45°C
5	48.05	0.23	-20.69	-21.71	-25.33	27.86	0.16	-20.27	-21.71	-23.50
10	60.83	0.25	-14.19	-18.41	-19.18	34.03	0.18	-20.15	-21.24	-23.81
15	48.26	0.20	-12.61	-12.78	-16.74	33.64	0.18	-19.63	-20.95	-23.22
20	11.02	0.07	-10.54	-11.60	-11.98	19.30	0.12	-16.47	-17.65	-18.87
25	34.62	0.15	-9.29	-10.88	-12.23	12.96	0.09	-14.21	-15.09	-16.03
30	20.69	0.10	-9.56	-10.64	-11.59	9.55	0.08	-13.24	-13.88	-14.78

doped gravel sand (Table 3), indicating that the calcined gravel sand had higher sorption capacity than iron-doped gravel sand.

### 3.5. Thermodynamic parameters

The thermodynamic parameters were analyzed with the following equations [28,43]:

$$K_D = \frac{C_0 - C_e}{C_e} \times \frac{V}{m} \quad (9)$$

$$\Delta G^\circ = -RT \ln (K_D) \quad (10)$$

$$\ln (K_D) = \frac{\Delta H^\circ}{RT} + \frac{\Delta S^\circ}{R} \quad (11)$$

where  $\Delta G^\circ$  (kJ mol<sup>-1</sup>) was the change in Gibb's free energy;  $\Delta S^\circ$  (kJ mol<sup>-1</sup> K<sup>-1</sup>) was the change in entropy;  $\Delta H^\circ$  (kJ mol<sup>-1</sup> K<sup>-1</sup>) was the change in enthalpy;  $K_D$  was the equilibrium constant (dimensionless);  $R$  (8.314 J mol<sup>-1</sup> K<sup>-1</sup>) was the gas constant;  $T$  (K) was absolute temperature;  $C_0$  (mg L<sup>-1</sup>) was the initial solution concentration;  $C_e$  (mg L<sup>-1</sup>) was the solution equilibrium concentration;  $V$  (mL) was the solution volume;  $m$  (g) was the mass of gravel sand.

The plot of  $\ln K_D$  vs.  $1,000/T$  according to Eq. (11) resulted in straight line with a slope  $\Delta H^\circ/R$  and an intercept  $\Delta S^\circ/R$  (Fig. 7). By substituting the value of  $R$ ,  $\Delta H^\circ$  and  $\Delta S^\circ$  were calculated (Table 4). Change of Gibbs energy,  $\Delta G^\circ$ , could be calculated by Eq. (10)

The calculation of thermodynamic parameters is helpful to elucidate sorption mechanisms. Depending on adsorbent and adsorbate, the sorption of phosphorus could increase or decrease with the increase of temperature [44].

The negative values of  $\Delta G^\circ$  (Table 4) indicated that the sorption of DIP was spontaneous [45]. The decrease of  $\Delta G^\circ$  with the increase of temperature

indicated a higher sorption impetus at higher temperature [46]. According to the comparison results of the samples of iron-doped gravel sand (G–Fe) and calcined gravel sand (G–C), the  $\Delta G^\circ$  value of G–C was smaller than that of G–Fe, confirming that the G–C had the higher sorption capacity than G–Fe. When  $\Delta G^\circ$  increases with the increase in inertial concentration, the sorption impetus decreased, indicating that desorption occurred more easily than sorption at the same temperature [47].

The positive value of  $\Delta S^\circ$  indicated an entropy-driven process. That is to say, molecular movement at the gravel sand/water interface turns more chaotic after sorption for water molecule desorption from gravel sand surface leads to the more chaotic movement from material surface to the solution.

The positive value of  $\Delta H^\circ$  for the sorption indicated that the process was the endothermic nature [48], and that the higher temperature was more conducive to sorption.

## 4. Conclusions

Sorption data suggested that two new materials (iron-doped gravel sand and calcined gravel sand) had higher sorption capacity to DIP than raw gravel sand and other common sorption materials. High pH was favorable for phosphorus sorption with calcined gravel sand, whereas low pH was beneficial to phosphorus sorption with iron-doped gravel sand. When initial phosphorus concentration increased, the phosphorus sorption capacity of the calcined gravel sand increased and the iron-doped gravel sand was relatively stable. The phosphorus removal efficiency of calcined gravel sand was higher than those of iron-doped gravel sand and raw gravel sand, and the removal efficiency decreased with the increase of phosphorus initial concentration. The equilibrium sorption data was better fitted by Langmuir isotherm.

The rate of sorption followed both the pseudo-first-order and pseudo-second-order models, and pseudo-second-order could better describe the sorption kinetics. According to the calculation of thermodynamic parameters for two new materials, the sorption was a feasible or spontaneous ( $\Delta G < 0$ ), random entropy-driven process ( $\Delta S > 0$ ), and endothermic ( $\Delta H > 0$ ) reaction. This study illustrates that these two new materials can be used as environment protection material in different fields due to their low cost.

### Acknowledgment

This work was supported by the Major Science and Technology Program for Water Pollution Control and Treatment, (No. 2012ZX07102-004 and 2012ZX07103-004).

### References

- [1] X.L. Huang, J.Z. Zhang, Phosphorus sorption on marine carbonate sediment: Phosphonate as Model Organic Compounds, *Chemosphere* 85 (2011) 1227–1232.
- [2] V. Baldy, M. Trémolières, M. Andrieu, J. Belliard, Changes in phosphorus content of two aquatic macrophytes according to water velocity, trophic status and time period in hardwater streams, *Hydrobiologia* 575 (2006) 343–351.
- [3] L.E. de-Bashan, Y. Bashan, Recent advances in removing phosphorus from wastewater and its future use as fertilizer (1997–2003), *Water Res.* 38 (2004) 4222–4246.
- [4] Z.F. Wang, M. Shi, J.H. Li, L. Zhou, Z.W. Wang, Z. Zheng, Sorption of dissolved inorganic and organic phosphorus compounds onto iron-doped ceramic sand, *Ecol. Eng.* 58 (2013) 286–295.
- [5] D.J. Currie, J. Kalff, The relative importance of bacterioplankton and phytoplankton in phosphorus uptake in freshwater, *Limnol. Oceanogr.* 29 (1984) 311–321.
- [6] K.G. Raghothama, Phosphate acquisition, *Annu. Rev. Plant Biol.* 50 (1999) 665–693.
- [7] J. Lin, Y. Zhan, Z. Zhu, Evaluation of sediment capping with active barrier systems (ABS) using calcite/zeolite mixtures to simultaneously manage phosphorus and ammonium release, *Sci. Total Environ.* 409 (2011) 638–646.
- [8] K. Sakadevan, H.J. Bavor, Phosphate adsorption characteristics of soils, slags and zeolite to be used as substrates in constructed wetland systems, *Water Res.* 32 (1998) 393–399.
- [9] J. Li, Y.-H. Zhan, J.-W. Lin, Effect of La-modified zeolite on phosphate sorption of Taihu Lake sediments, *J. Ecol. Rural Environ.* 29 (2013) 500–506.
- [10] G.M. Ayoub, B. Koopman, N. Pandya, Iron and aluminum hydroxy (oxide) coated filter media for low-concentration phosphorus removal, *Water Environ. Res.* 73 (2001) 478–485.
- [11] J. Bouzid, Z. Elouear, M. Ksibi, M. Feki, A. Montiel, A study on removal characteristics of copper from aqueous solution by sewage sludge and pomace ashes, *J. Hazard. Mater.* 152 (2008) 838–845.
- [12] N. Boujelben, F. Bouhamed, Z. Elouear, J. Bouzid, M. Feki, Removal of phosphorus ions from aqueous solutions using manganese-oxide-coated sand and brick, *Desalin. Water Treat.* 52 (2014) 2282–2292.
- [13] K. Riahi, B. Ben Thayer, A. Ben Mammou, A. Ben Ammar, M.H. Jaafoura, Biosorption characteristics of phosphates from aqueous solution onto *Phoenix dactylifera* L. date palm fibers, *J. Hazard. Mater.* 170 (2009) 511–519.
- [14] M.A. Wahab, R. Ben Hassine, S. Jellali, *Posidonia oceanica* (L.) fibers as a potential low-cost adsorbent for the removal and recovery of orthophosphate, *J. Hazard. Mater.* 191 (2011) 333–341.
- [15] S. Jaouadi, M.A. Wahab, M. Anane, L. Bousselmi, S. Jellali, Powdered marble wastes reuse as a low-cost material for phosphorus removal from aqueous solutions under dynamic conditions, *Desalin. Water Treat.* 52 (2014) 1705–1715.
- [16] A.J. Erickson, J.S. Gulliver, P.T. Weiss, Capturing phosphates with iron enhanced sand filtration, *Water Res.* 46 (2012) 3032–3042.
- [17] D.M.R. Mateus, M.M.N. Vaz, H.J.O. Pinho, Fragmented limestone wastes as a constructed wetland substrate for phosphorus removal, *Ecol. Eng.* 41 (2012) 65–69.
- [18] I.R. Lantzke, A.D. Heritage, G. Pistillo, D.S. Mitchell, Phosphorus removal rates in bucket size planted wetlands with a vertical hydraulic flow, *Water Res.* 32 (1998) 1280–1286.
- [19] H. Habte Lemji, H. Eckstädt, A pilot scale trickling filter with pebble gravel as media and its performance to remove chemical oxygen demand from synthetic brewery wastewater, *J. Zhejiang Univ. Sci. B* 14 (2013) 924–933.
- [20] J. Murphy, J.P. Riley, A modified single solution method for the determination of phosphate in natural waters, *Anal. Chim. Acta* 27 (1962) 31–36.
- [21] A. Zhou, H. Tang, D. Wang, Phosphorus adsorption on natural sediments: Modeling and effects of pH and sediment composition, *Water Res.* 39 (2005) 1245–1254.
- [22] A. Rey, M. Faraldos, J.A. Casas, J.A. Zazo, A. Bahamonde, J.J. Rodríguez, Catalytic wet peroxide oxidation of phenol over Fe/AC catalysts: Influence of iron precursor and activated carbon surface, *Appl. Catal., B* 86 (2009) 69–77.
- [23] M.M. Maroto-Valer, I. Dranca, T. Lupascu, R. Nastas, Effect of adsorbate polarity on thermodesorption profiles from oxidized and metal-impregnated activated carbons, *Carbon* 42 (2004) 2655–2659.
- [24] G. Muñoz, V. Fierro, A. Celzard, G. Furdin, G. Gonzalez-Sánchez, M.L. Ballinas, Synthesis, characterization and performance in arsenic removal of iron-doped activated carbons prepared by impregnation with Fe(III) and Fe(II), *J. Hazard. Mater.* 165 (2009) 893–902.
- [25] J. Berkowitz, M.A. Anderson, R.C. Graham, Laboratory investigation of aluminum solubility and solid-phase properties following alum treatment of lake waters, *Water Res.* 39 (2005) 3918–3928.
- [26] F. Ying, Y. Shui-li, Characterization and phosphorus removal of poly-silicic-ferric coagulant, *Desalination* 247 (2009) 442–455.
- [27] R. Al-Oweini, H. El-Rassy, Synthesis and characterization by FTIR spectroscopy of silica aerogels prepared

- using several  $\text{Si(OR)}_4$  and  $\text{R}'\text{Si(OR)}_3$  precursors, *J. Mol. Struct.* 919 (2009) 140–145.
- [28] S.-Y. Yoon, C.-G. Lee, J.-A. Park, J.-H. Kim, S.-B. Kim, S.-H. Lee, J.-W. Choi, Kinetic, equilibrium and thermodynamic studies for phosphate adsorption to magnetic iron oxide nanoparticles, *Chem. Eng. J.* 236 (2014) 341–347.
- [29] Y. Yang, Y. Zhao, A. Babatunde, L. Wang, Y. Ren, Y. Han, Characteristics and mechanisms of phosphate adsorption on dewatered alum sludge, *Sep. Purif. Technol.* 51 (2006) 193–200.
- [30] S.S.S. Rajan, Adsorption of divalent phosphate on hydrous aluminium oxide, *Nature* 253 (1975) 434–436.
- [31] N.Y. Mezenner, A. Bensmaili, Kinetics and thermodynamic study of phosphate adsorption on iron hydroxide-eggshell waste, *Chem. Eng. J.* 147 (2009) 87–96.
- [32] B. Kostura, H. Kulveitová, J. Leško, Blast furnace slags as sorbents of phosphate from water solutions, *Water Res.* 39 (2005) 1795–1802.
- [33] H. Ye, F. Chen, Y. Sheng, G. Sheng, J. Fu, Adsorption of phosphate from aqueous solution onto modified palygorskites, *Sep. Purif. Technol.* 50 (2006) 283–290.
- [34] C. Sairam Sundaram, N. Viswanathan, S. Meenakshi, Uptake of fluoride by nano-hydroxyapatite/chitosan, a bioinorganic composite, *Bioresour. Technol.* 99 (2008) 8226–8230.
- [35] A. Fouladi Tajar, T. Kaghazchi, M. Soleimani, Adsorption of cadmium from aqueous solutions on sulfurized activated carbon prepared from nut shells, *J. Hazard. Mater.* 165 (2009) 1159–1164.
- [36] A. Drizo, C.A. Frost, J. Grace, K.A. Smith, Physico-chemical screening of phosphate-removing substrates for use in constructed wetland systems, *Water Res.* 33 (1999) 3595–3602.
- [37] C.A. Arias, M. Del Bubba, H. Brix, Phosphorus removal by sands for use as media in subsurface flow constructed reed beds, *Water Res.* 35 (2001) 1159–1168.
- [38] R.H. Li, C. Kelly, R. Keegan, L.W. Xiao, L. Morrison, X.M. Zhan, Phosphorus removal from wastewater using natural pyrrhotite, *Colloids Surf., A* 427 (2013) 13–18.
- [39] P. Janoš, P. Michálek, L. Turek, Sorption of ionic dyes onto untreated low-rank coal—Oxihumolite: A kinetic study, *Dyes Pigm.* 74 (2007) 363–370.
- [40] Y. Onganer, Ç. Temur (Işık), Adsorption dynamics of Fe(III) from aqueous solutions onto activated carbon, *J. Colloid Interface Sci.* 205 (1998) 241–244.
- [41] Y.S. Ho, G. McKay, Pseudo-second order model for sorption processes, *Process Biochem.* 34 (1999) 451–465.
- [42] C. Ding, X. Yang, W. Liu, Y. Chang, C. Shang, Removal of natural organic matter using surfactant-modified iron oxide-coated sand, *J. Hazard. Mater.* 174 (2010) 567–572.
- [43] C. Namasivayam, D. Sangeetha, Equilibrium and kinetic studies of adsorption of phosphate onto  $\text{ZnCl}_2$  activated coir pith carbon, *J. Colloid Interface Sci.* 280 (2004) 359–365.
- [44] M. Cea, J.C. Seaman, A. Jara, M.L. Mora, M.C. Diez, Kinetic and thermodynamic study of chlorophenol sorption in an allophanic soil, *Chemosphere* 78 (2010) 86–91.
- [45] L. Huang, L. Fu, C. Jin, G. Gielen, X. Lin, H. Wang, Y. Zhang, Effect of temperature on phosphorus sorption to sediments from shallow eutrophic lakes, *Ecol. Eng.* 37 (2011) 1515–1522.
- [46] K. Li, Z. Zheng, X. Huang, G. Zhao, J. Feng, J. Zhang, Equilibrium, kinetic and thermodynamic studies on the adsorption of 2-nitroaniline onto activated carbon prepared from cotton stalk fibre, *J. Hazard. Mater.* 166 (2009) 213–220.
- [47] D. Kim, Adsorption characteristics of Fe(III) and Fe(III)–NTA complex on granular activated carbon, *J. Hazard. Mater.* 106 (2004) 67–84.
- [48] G. Alagumuthu, M. Rajan, Equilibrium and kinetics of adsorption of fluoride onto zirconium impregnated cashew nut shell carbon, *Chem. Eng. J.* 158 (2010) 451–457.